A comparison of new and existing equations for estimating sensible heat flux using surface renewal and similarity concepts

F. Castellví,[1] R. L. Snyder,[2] D. D. Baldocchi,[3] and A. Martínez-Cob[4]

Received 5 October 2005; revised 10 April 2006; accepted 20 April 2006; published 5 August 2006.

[1] This paper describes two approaches for estimating sensible heat flux, using surface renewal and similarity concepts. One approach depends on a temperature structure function parameter and is valid in the inertial sublayer. The other approach depends on the temperature standard deviation and operates when measurements are made above the canopy top, either in the roughness or inertial sublayer. The approaches were tested over grass, rangeland grass, wheat, grape vineyard, and nectarine and olive orchards. It is shown that the free convection limit expression for the standard deviation method holds for slightly unstable conditions. When surface homogeneity and fetch requirements are not fully met in the field, the results show that the equations based on surface renewal principles are more robust and accurate than equations exclusively based on similarity backgrounds. It is likely that the two methods are less sensitive to site-specific adjustment of the similarity relationships unless the canopy is rather heterogeneous. Under unstable conditions, the free convection limit equation, which depends on the temperature standard deviation, can provide online sensible heat flux estimates using affordable battery-powered data logger with temperature data as the only input. The approach performed well when measuring above the canopy in the roughness and inertial sublayers, thus suggesting that the method is useful for long-term monitoring over growing vegetation.

Citation: Castellví, F., R. L. Snyder, D. D. Baldocchi, and A. Martínez-Cob (2006), A comparison of new and existing equations for estimating sensible heat flux using surface renewal and similarity concepts, *Water Resour. Res.*, *42*, W08406, doi:10.1029/2005WR004642.

1. Introduction

[2] The use of lysimeters or the eddy covariance method for measuring latent heat flux is limited by the relatively high cost of both instruments and maintenance. It is therefore desirable to obtain indirect estimates using low-cost and robust instrumentation. For estimating sensible heat flux, H, the surface renewal (SR) method [*Higbie*, 1935] in conjunction with the analysis of air temperature traces for estimating H over natural surfaces [*Paw U et al.*, 1995, 2005] is attractive because it avoids many of the difficulties associated with similarity principles and it is less expensive. The SR analysis is applicable close to the surface thus making easier the access to instrumentation over tall canopies, and because of lower cost, spatial replication is less expensive than with other methods. For water management, SR analysis for estimating H is attractive because, through a surface energy balance closure, latent heat flux can be estimated as the residual of the energy balance equation [*Anderson et al.*, 2003].

[3] In the earlier SR method calibration to account for unequal heating below the sensor height is required [*Snyder et al.*, 1996; *Spano et al.*, 1997; *Zapata and Martínez-Cob*, 2001; *Castellví*, 2004]. Our goal was to automatically account for calibration coefficient changes, to keep instrumentation simple, inexpensive and accessible, and to avoid problems associated with large data sets. Two new approaches for estimating H using SR analysis were derived assuming ideal field conditions (i.e., a flat, extensive and homogeneous surface); however, such conditions are frequently not met in field trials. Therefore method performance was also tested over heterogeneous canopies. One of these two new approaches, which depends on the standard deviation and the third-order structure function of the temperature, produced reliable results from data recorded in either the inertial or roughness sublayers and it was simple enough to allow online data logger calculation of H under unstable atmospheric conditions.

2. Methods

2.1. Theory and Short Background

[4] SR analysis assumes that turbulent exchange of a scalar is driven by the regular replacement of the air parcel in contact with the surface where the exchange occurs. As one air parcel sweeps down to the surface, it replaces

[1]Departamento de Medi Ambient i Cienciès del Sòl, University of Lleida, Lleida, Spain.
[2]Department of Land, Air and Water Resources, University of California, Davis, California, USA.
[3]Department of Environmental Science, Policy and Management, University of California, Berkeley, California, USA.
[4]Departamento de Genética y Producción Vegetal, Estación Experimental de Aula Dei, Consejo Superior de Investigaciones Científicas, Zragoza, Spain.

0043-1397/06/2005WR004642

another that is ejected from the canopy, once the latter has enriched or depleted the scalar. SR models are based on the fact that most of the turbulent transfer is associated with large-scale coherent eddies, which are evident as scalar ramp time series. An ideal and comprehensive scheme for this process was originally presented by *Paw U et al.* [1995] and *Chen et al.* [1997a] (see Figure A1). Sensible heat flux from the surface at height, z (within the canopy, in the roughness or inertial sublayer), over the averaging period (commonly half hour) is determined by the following expression [see, e.g., *Paw U et al.*, 1995; *Snyder et al.*, 1996; *Chen et al.*, 1997a; *Spano et al.*, 2000]

$$H = (\alpha z)\rho C_p \frac{A}{\tau} \tag{1}$$

To shorten the paper, definitions of symbols are provided in Table 1. A practical method for estimating ramp dimensions according to ramp model shown in Figure A1 [*Chen et al.*, 1997a] is presented in Appendix A. In equation (1) the variable (αz) is the volume of air, with height z per unit ground area, exchanged on average for each ramp in the sample period. Assuming as z the height of the air parcel to be renewed, parameter α accounts for the unequal heating from the bottom to the top of the renewed air parcel [*Paw U et al.*, 1995]. In the work by *Castellví* [2004], the variable (αz) represents the mean eddy size responsible for the renewal process that fits the local air temperature gradient and the following relationship was proposed when measuring above the canopy:

$$\frac{A}{(\alpha z)} \propto \frac{dT}{dz} = \begin{cases} \beta \dfrac{A}{(z-d)} & z > z^* \\ \beta \dfrac{A}{z} & h \le z \le z^* \end{cases} \tag{2}$$

The parameter β is a dimensionless aerodynamic resistance of the number of ramps formed during a given period, and z* is the roughness sublayer depth. In (2) the eddy size was scaled as, (z − d) and z for measurements well above and close to the canopy, respectively [*Kaimal and Finnigan*, 1994; *Chen et al.*, 1997b]. Following *Castellví* [2004], parameters α and β are estimated as

$$\alpha = \begin{cases} \left[\dfrac{k}{\pi}\dfrac{(z-d)}{z^2}\dfrac{\tau u_*}{\phi_h(\varsigma)}\right]^{1/2} & z > z^* \\ \left[\dfrac{k}{\pi}\dfrac{z^*}{z^2}\dfrac{\tau u_*}{\phi_h(\varsigma)}\right]^{1/2} & h \le z \le z^* \end{cases} \tag{3}$$

$$\alpha\beta = \begin{cases} \dfrac{(z-d)}{z\pi} & z > z^* \\ \dfrac{1}{\pi} & h \le z \le z^* \end{cases} \tag{4}$$

The Obukhov length, L_o, is defined

$$L_O = \frac{u_*^3}{\left(\frac{kg}{\rho}\right)\left(\frac{H}{TC_p} + 0.61E\right)} \approx -\rho C_p \frac{u_*^3}{\left(\frac{kg}{T}\right)H} \tag{5}$$

where the right-hand expression is traditionally used for dry climates. Combining equations (1), (3), (5) and (A5) from Appendix A gives the following equation for estimating sensible heat flux [*Castellví*, 2004]

$$H = \begin{cases} \rho C_p \left(\dfrac{g}{T}\right)^{1/5} \dfrac{(k(z-d))^{4/5}}{\pi^{3/5}} \left(-\gamma^3 \dfrac{S^3_{(rx)}}{r_x}\right)^{3/5} A^{-3/5} \left(\dfrac{\phi_h^{-3}(\varsigma)}{-\varsigma}\right)^{1/5} & z > z^* \\ \rho C_p \left(\dfrac{g}{T}\right)^{1/5} k^{4/5} \left(\dfrac{z^*}{\pi}\right)^{3/5} z^{1/5} \left(-\gamma^3 \dfrac{S^3_{(rx)}}{r_x}\right)^{3/5} A^{-3/5} \left(\dfrac{\phi_h^{-3}(\varsigma)}{-\varsigma}\right)^{1/5} & h \le z \le z^* \end{cases} \tag{6}$$

2.2. Method Description

[5] Combining equations (1), (5), and (A5), the friction velocity for dry climates can be expressed as

$$u_* = \begin{cases} \left[\alpha\gamma^3 (z-d) z \dfrac{kg}{TA^2}\left(\dfrac{S^3_{(r_x)}}{r_x}\right)\right]^{1/3} \dfrac{1}{\varsigma^{1/3}} & z > z^* \\ \left[\alpha\gamma^3 z^2 \dfrac{kg}{TA^2}\left(\dfrac{S^3_{(r_x)}}{r_x}\right)\right]^{1/3} \dfrac{1}{\varsigma^{1/3}} & h \le z \le z^* \end{cases} \tag{7}$$

Combining equations (3) and (7), friction velocity can be rewritten as

$$u_* = \begin{cases} \left[\left(\dfrac{g}{T}\right)^2 (k(z-d))^3 \dfrac{\gamma^3}{\pi} A^{-1}\left(-\dfrac{S^3_{(r_x)}}{r_x}\right)\right]^{1/5} \left(\varsigma^2 \phi_h(\varsigma)\right)^{-1/5} & z > z^* \\ \left[\left(\dfrac{g}{T}\right)^2 (k^3 z^2 z^*) \dfrac{\gamma^3}{\pi} A^{-1}\left(-\dfrac{S^3_{(r_x)}}{r_x}\right)\right]^{1/5} \left(\varsigma^2 \phi_h(\varsigma)\right)^{-1/5} & h \le z \le z^* \end{cases} \tag{8}$$

Equation (8) is consistent with the parameters needed to describe turbulence under convective conditions, i.e., as turbulence becomes independent from the stability parameter and friction velocity. The function $(\zeta^2\phi_h(\zeta))^{-1/5}$ can be approximated as a constant with a value of 1.2 that produces relative errors of less than 10% for $\zeta \le -1$. For free convection, according to *Högström* [1990], equation (8) tends to be decoupled from the surface since the ramp dimensions are greatly influenced by the boundary layer scale eddies. Under near neutral conditions, both ζ and $S^3_{(r)}$ tend to 0, giving a finite value.

2.2.1. Measuring in the Inertial Sublayer

[6] Monin-Obukhov similarity theory holds for measurements in the inertial sublayer and it is known that

$$\frac{(z-d)}{T_*}\frac{dT}{dz} = k^{-1}\phi_h(\zeta) \tag{9}$$

Using equations (2) and (9), an expression that combines surface renewal with similarity concepts is

$$\frac{A}{T_*} = (k\beta)^{-1}\phi_h(\zeta) \tag{10}$$

Table 1. Glossary of Symbols

Symbol	Definition
A	mean ramp amplitude
C_p	specific heat of air at constant pressure
C_{tt}	temperature structure function parameter
d	zero-plane displacement
D	mean free space between roughness elements
g	acceleration due to gravity
$g_1(\zeta) = \begin{bmatrix} 4.9(1-7\varsigma)^{-2/3} & \zeta < 0 \\ 4.9 & \zeta = 0 \\ 4.9(1+2.75\xi) & \zeta > 0 \end{bmatrix}$	empirical similarity-based relationship (valid in the inertial sublayer), *Wyngaard et al.* [1971]
$g_2(\zeta) = \begin{bmatrix} 0.95(0.05-\varsigma)^{-1/3} & \zeta 0 \\ 2.5 & \zeta = 0 \\ -2(\text{uncertain}) & \zeta > 0 \end{bmatrix}$	empirical similarity-based relationship (valid in the inertial sublayer), *Tillman* [1972]
$g_2^*(\zeta)$	$g_2(\zeta)$ valid in the roughness sublayer
h	canopy height
H	sensible heat flux
Hec	sensible heat flux measured with the eddy covariance
K	Von Kármán constant
K_h	turbulent eddy diffusion for heat valid in the inertial sublayer
Kh^*	turbulent eddy diffusion for heat valid in the roughness sublayer
L_0	Obukov length
N	number of observations
r_x	time lag that maximizes $(S^3(r)/r)$
$\text{RMSE} = \left[\frac{\sum_{i=1}^{N}(y_i-x_i)^2}{N}\right]^{1/2}$	root-mean-square error
$\text{RMSEs} = \left[\frac{\sum_{i=1}^{N}(\bar{y}_i-x_i)^2}{N}\right]^{1/2}$	systematic root mean square error
$\text{RMSEu} = \left[\frac{\sum_{i=1}^{N}(y_i-\bar{y}_i)^2}{N}\right]^{1/2}$	unsystematic root-mean-square error
R^2	coefficient of determination
$S^n(r)$	structure functions for SR analysis, equation (A1)
T	mean absolute air temperature
T_*	surface temperature scale
UE	unsystematic portion of RMSE^2
u_*	friction velocity
X	independent variable (measurement)
Y	dependent variable (estimate)
$\bar{y} = ax + b$	predicted value (from the linear fitting $y = a + b\,x$) for the dependent variable
Z	measurement height
Z^*	roughness sublayer depth
α	parameter in equation (1)
β	parameter in equation (2)
$\phi_h(\zeta) = \begin{bmatrix} 0.74/\sqrt{1-9\zeta} & \zeta 0 \\ 0.74 & \zeta = 0 \\ 0.74+5\zeta & \zeta > 0 \end{bmatrix}$	stability function for heat transfer (valid in the inertial sublayer), *Businger et al.* [1971]
$\phi_h^*(\zeta)$	stability function for heat transfer (valid in the roughness sublayer)
γ	parameter in equation (A5)
ρ	air density
σ_T	air temperature standard deviation
τ	mean inverse ramp frequency
$\zeta = (z-d)/L_O$	stability parameter

Two well-established similarity relationships ($g_1(\zeta)$ and $g_2(\zeta)$), which also involve T_*, were originally given by *Wyngaard et al.* [1971] and *Tillman* [1972] as

$$\frac{C_{tt}}{T_*^2} = (z-d)^{-2/3} g_1(\varsigma) \tag{11}$$

$$\frac{\sigma_T}{T_*} = g_2(\varsigma) \tag{12}$$

respectively. Equations (10), (11), (12), and (7) are used to express the sensible heat flux ($H = \rho C_p T_* u_*$) in two different forms:

[7] When the temperature structure function parameter, C_{tt}, is known:

$$H = \rho C_p \left[\gamma^3 (z-d)^{4/3} \frac{kgz}{T} C_{tt}^{1/2} \left(-\frac{S_{r_x}^3}{r_x}\right)\right]^{1/3} \cdot \left(\alpha (k\beta)^2 \frac{\phi_h^{-2}(\zeta) g_1^{-1/2}(\zeta)}{-\zeta}\right)^{1/3} \tag{13}$$

When the temperature standard deviation, σ_T, is known:

$$H = \rho C_p \left[\gamma^3 (z-d) \frac{kgz}{T} \sigma_T \left(-\frac{S_{r_x}^3}{r_x}\right)\right]^{1/3} \cdot \left(\alpha (k\beta)^2 \frac{\phi_h^{-2}(\zeta) g_2^{-1}(\zeta)}{-\zeta}\right)^{1/3} \tag{14}$$

2.2.2. Measuring Above the Canopy in the Roughness Sublayer

[8] Within this region, similarity-based relationships may be invalid. On the basis of flux-gradient relationships for homogeneous canopies, sensible heat flux can be estimated using the expression, $H = \rho C_p K_h^* dT/dz$, where K_h^* is the eddy diffusivity for heat in the roughness sublayer [*Cellier and Brunet*, 1992]. Denoting $\phi_h^*(\zeta)$ as an appropriate stability function for heat in the roughness sublayer, *Cellier and Brunet* [1992] found the following relationship: $\phi_h^*(\zeta)/\phi_h(\zeta) = K_h/K_h^* \sim (z-d)/z^*$. Since $K_h = ku_*(z-d)\phi_h^{-1}(\zeta)$ is a suitable expression for the eddy diffusivity for heat in the inertial sublayer [*Brutsaert*, 1982], it follows that the eddy diffusivity for heat in the roughness sublayer can be estimated as

$$K_h^* = k\, u_* z^* \phi_h^{-1}(\zeta) \tag{15}$$

Assuming that the ratio of similarity relationships in equations (10) and (12), $\phi_h(\zeta)/g_2(\zeta)$, also holds true in the roughness sublayer through a given proportionality, μ, as

$$\frac{(k\beta)A}{\sigma_r} = \left(\frac{\phi_h(\zeta)}{g_2(\zeta)}\right) = \mu \left(\frac{\phi_h^*(\zeta)}{g_2^*(\zeta)}\right) \tag{16}$$

where $g_2^*(\zeta)$ denotes the corresponding $g_2(\zeta)$ valid in the roughness sublayer. The assumption made in the second equality of equation (16) is supported by the literature. *Lloyd et al.* [1991] found that the form of $g_2(\zeta)$ is independent of the terrain type; *Hsieh et al.* [1996] and *Wesson et al.* [2001] found that $g_2^*(\zeta)$ for nonuniform surfaces is proportional to $g_2(\zeta)$. *Cellier and Brunet* [1992] and *Hsieh et al.* [1996] found that the form of $\phi_h(\zeta)$ is rather robust to nonuniform ground heating condition. Combining equations (2), (7), (15), (16) and $H = \rho C_p K_h^* dT/dz$ gives the following expression for estimating the sensible heat flux in the roughness sublayer:

$$H = \rho C_p \left[\frac{(\gamma z^*)^3}{z} \frac{kg}{T} \sigma_T \left(-\frac{S_{r_x}^3}{r_x}\right)\right]^{1/3} \cdot \left(\alpha (k\beta)^2 \frac{\phi_h^{-2}(\zeta) g_2^{-1}(\zeta)}{-\zeta}\right)^{1/3} \quad h \le z \le z^* \tag{17}$$

where the parameter μ, in equation (16), was set equal to 1.0 for practical application. Equation (16) was obtained after equating T_* from equations (10) and (12), so it was expected that the portion μ be a constant close to the unity. The dependence in equation (17) on parameter μ is through the power 1/3. Then, if μ slightly departs from 1.0, the total error introduced in H is diminished.

2.2.3. Dependence of Equations (13), (14), and (17) on the Stability Parameter

[9] This requires experimental evidence. In Appendix B, according to our data set, it is shown that: (1) under slightly unstable conditions, the three equations permit estimation of H from air temperature measurements, (2) under moderately stable conditions, wind speed measurement is required, and (3) under strong stability conditions, the equations depend only on temperature measurements, although may be uncertain. Appendix B shows that under unstable conditions, the different expressions permit H estimation as follows.

[10] When the temperature structure function parameter is known,

$$H = \rho C_p \left(1.65\gamma \frac{k^{5/6} g^{1/3}}{\pi^{1/2}}\right)(z-d)^{7/9} \cdot \left[\frac{C_{tt}^{1/2}}{T}\left(-\frac{S_{r_x}^3}{r_x}\right)\right]^{1/3} \quad z \ge z^* \tag{18}$$

When the temperature standard deviation is known,

$$H = \begin{cases} \rho C_p \left(1.65\gamma \dfrac{k^{5/6} g^{1/3}}{\pi^{1/2}}\right)(z-d)^{2/3} \left[\dfrac{\sigma_T}{T}\left(-\dfrac{S_{r_x}^3}{r_x}\right)\right]^{1/3} & z \ge z^* \\ \rho C_p \left(1.65\gamma \dfrac{k^{5/6} g^{1/3}}{\pi^{1/2}}\right) z^{1/6} (z^*)^{1/2} \left[\dfrac{\sigma_T}{T}\left(-\dfrac{S_{r_x}^3}{r_x}\right)\right]^{1/3} & h \le z \le z^* \end{cases} \tag{19}$$

Equations (18) and (19) express the free convection limit approaches for equations (13), (14) and (17), respectively. According to Appendix B the free convection limit is reached for $\zeta \le -0.1$, although it likely may hold for a wider range. This requires experimental evidence. The free convection limit for equation (6) holds in the interval, $-3 \le \zeta \le -0.03$, with a relative error of less than 8.5% [*Castellví*,

2004]. Therefore, when the ramp amplitude is known, the sensible heat flux can be estimated as

$$H = \begin{cases} \rho C_p \left(2.4\gamma^{9/5}\frac{k^{4/5}g^{1/5}}{\pi^{3/5}}\right)\left[\frac{(z-d)^4}{T}\right]^{1/5}\left(-\frac{S^3_{(rx)}}{r_x}\right)^{3/5}A^{-3/5} & z > z^* \\ \rho C_p \left(2.4\gamma^{9/5}\frac{k^{4/5}g^{1/5}}{\pi^{3/5}}\right)\left[z\frac{(z^*)^3}{T}\right]^{1/5}\left(-\frac{S^3_{(rx)}}{r_x}\right)^{3/5}A^{-3/5} & h \le z \le z^*. \end{cases} \quad (20)$$

For applying equations (18), (19) and (20), previous knowledge of the atmospheric stability condition of the surface layer during each sample is required. The sign of the third moment of the temperature structure function coincides with the sign of the stability parameter, see (A5) [*Van Atta*, 1977; *Antonia et al.*, 1981].

2.3. Existing Similarity-Based Equations for Estimating Sensible Heat Flux

[11] The main objective was to analyze the performance of the new approaches for estimating sensible heat flux. It is interesting, however, to examine the performance of several other equations from the literature; especially those requiring the same measurements. Thus we compare the new method with the similarity-based expressions originally presented by *Wyngaard et al.* [1971] and *Tillman* [1972] for estimating sensible heat flux that involve the temperature structure function parameter and the temperature standard deviation, respectively:

$$H = \rho C_p \left(\frac{kg}{T}\right)^{1/2}(z-d)\left(\frac{(g_1(\varsigma))^{-3/2}}{-\varsigma}\right)^{1/2}(C_{tt})^{3/4} \qquad z > z^* \quad (21)$$

$$H = \rho C_p \left(\frac{kg(z-d)}{T}\right)^{1/2}\left(\frac{(g_2(\varsigma))^{-3}}{-\varsigma}\right)^{1/2}(\sigma_T)^{3/2} \qquad z > z^* \quad (22)$$

respectively. The respective free convection limit approach, for the two equations, is as follows:

$$H = \rho C_p \left(0.8(kg)^{1/2}\right)\frac{(z-d)}{T^{1/2}}(C_{tt})^{3/4} \quad \varsigma \ll -0.14 \quad (23)$$

$$H = \rho C_p \left(1.08(kg)^{1/2}\right)\left(\frac{(z-d)}{T}\right)^{1/2}(\sigma_T)^{3/2} \quad \varsigma < -0.04 \quad (24)$$

2.4. Advantages, Limitations, Minimum Instrumentation, and Data Processing Requirements

2.4.1. Advantages and Limitations for Field Applications

[12] Equations (6), (13), (14), (21), and (22) operate when measurements are made in the inertial sublayer. Equations (6) and (17) operate in the roughness sublayer and therefore are useful when fetch and accessibility to sensors are a limitation. All six equations are comparable in terms of input data. However, their respective free convection limit approaches are not comparable. For determining the temperature structure function parameter in equations (18) and (23), a minimum of two thermocouples or a thermocouple and a cup anemometer in conjunction with the Taylor hypothesis of frozen turbulence is required. The other free convection limit approaches, using equations (19), (20) and (24), require a single thermocouple.

[13] Equations (19) and (24) are directly comparable. Because previous knowledge of the surface layer atmospheric stability is required, if the sign of a third-order temperature structure function is used to identify unstable conditions, then the same calculations are needed for equations (19) and (24). Equation (24), however, is not necessarily valid when measurements are made close to the canopy top.

[14] Equations (6), (13), (14), (17), (21) and (22) need to be solved on a computer because they depend on the stability parameter. Sensible heat flux from equation (20) cannot be recorded online using slow data loggers. The ramp amplitude computation is needed, and data logger speed limits processing of the high-frequency temperature data.

[15] Overall, depending on the required accuracy, equation (19) is likely adequate under unstable conditions. A single thermocouple is required and measurements can be taken close to or well above the canopy top.

2.4.2. Minimum Instrumentation and Data Processing Requirements

[16] Equations (19) and (24) require a fine-wire thermocouple and a data logger for estimating H under unstable conditions. Thermocouples with smaller diameter are more responsive and more accurate, but thermocouples with larger diameter are less prone to damage. *Duce et al.* [1998] reported that half-hourly structure functions determined with different diameter wire size affected the ramp parameter determination. Thermocouples with about 7.6×10^{-5} m diameter are proved to give good performance [*Snyder et al.*, 1996; *Spano et al.*, 1997, 2000] and are infrequently damaged by rainfall and other events.

[17] A data logger capable of storing half-hourly temperature standard deviations and the third-order structure function for several time lags is required. Generally, three time lags are sufficient if a reasonable estimate of time lag r_x is available (see Table A1). The sampling frequency requirement is limited mainly by the processing time needed between samples. The appropriate sampling frequency depends on the canopy size and how close to the canopy top the measurements are taken. For example, tall and dense forest canopies could be monitored using a frequency of about 4 Hz. For moderate tall, sparse or dense canopies (e.g., nectarine or olive orchard as described next), near canopy top measurements with time lags of about 0.5 s and 4 Hz measuring frequency may be adequate. For shorter canopies (e.g., grasses, wheat, etc.), it is better to measure 0.5 to 1.0 m above the canopy top [*Snyder et al.*, 1996].

Table 2. Summary of the Experimental Sites[a]

Description	Experiment					
	1	2	3	4	5	6
Surface	grass	wheat	vineyard	rangeland grass	nectarines	olives
Location	Davis, California	Davis, California	Oakville, California	Ione, California	Portugal	Spain
Canopy height, m	0.10	0.70	2.00	0.25	3.20	3.50
d/z*, m	0.067/–	0.47/1.2	1.34/5.5	0.167/–	2.14/9.5	0/12.0
Homogeneous	yes	yes	no	yes	no	no
Fetch, m	50	>400	>300	>200	>350	550
Instrument height, m						
Instrument T	0.6	0.7	2.0	–	3.2	3.5
	0.7	1.0	2.3			5.1
	0.9	1.3	2.6			
	1.2		2.9			
	1.0					
	1.3					
Instrument 1D	0.6	1.0	3.0	–	3.5	–
	0.7					
Instrument 3D	–	–	–	2.0	–	4.9
Instrument W	2.0	2.0	3.0	–	–	–
Range of H, W m^{-2}	−77 to 125	80 to 322	45 to 326	−78 to 473	−47 to 264	−98 to 416
Half-hour samples						
Stable	261	–	–	2179	57	1887
Unstable	317	43	133	3843	69	1907

[a]Instruments are T, thermocouple (7.6×10^{-5} m diameter) measuring temperature at 8 Hz, except for the olive orchard that was 4 Hz; 1D, omnidimensional sonic anemometer (Campbell Scientific Inc., CSI) measuring vertical wind speed and temperature at 10 Hz; 3D, three-dimensional sonic anemometer (CSI expect for rangeland grass that was a Gill Masterwind Pro) measuring the three wind components and virtual temperature at 10 Hz; W, cup anemometer measuring half-hour wind speed. The fetch corresponds to edge distance in the mean stream-wind direction. The zero plane displacement, d, and roughness depth, z*, were both estimated (see text).

Appropriate time lags are about 0.2 s; therefore sampling frequencies of 8 Hz are suitable [*Castellví*, 2004]. Under windy conditions, higher-frequency measurements might be needed because of the high absorption of momentum.

[18] During near neutral and stable conditions, ramps are often not in agreement with the sign of the measured H; however, it is a minor problem because the H values are typically low. Therefore measurement frequencies greater than 4–8 Hz are unnecessary for most field applications under unstable conditions. A data logger such as a Campbell Scientific, Inc. CR10X meets the requirements to collect the standard deviation and 3rd moment for several time lags. With this data logger, computation of temperature differences for three different time lags in order to obtain three half-hour structure functions requires an execution time of 0.136 s. Then, the minimum possible time execution interval to be implemented in a CR10X would be 0.15625 s (6.4 Hz), and three half-hour structure functions, corresponding to time lags of 0.15625 s, 0.46875 s and 0.625 s, could be computed and stored in data logger memory, allowing online H calculation.

[19] Online computation of latent heat flux through a simplified surface energy balance [*Allen et al.*, 1996] could be implemented when additional instrumentation for measuring half-hour net radiation, wind speed and direction, and soil heat flux (using two soil heat flux plates and a soil-averaging temperature sensor), is also connected to the same CR10X data logger. However, in some instances, storing these other parameters online can lead to small errors due to inadequate data logger computational speed. Generally, such errors will have minimal effect on the H estimate or LE estimates. Using a CR10X, an execution time interval of 6.4 Hz would not be enough for accomplishing all computation steps required: every half-hour, between 1 and 7% of the temperature differences calculated for structure function computation would be missed or not accurately computed, depending on time lag considered. These errors in H calculation would be small in general, however, to avoid such situations, the alternatives are (1) use of two CR10X data loggers, one for online H computation and the other for recording the other variables required for the energy balance closure; (2) use of a single CR10X data logger with a higher time execution interval, for instance, 0.25 s (4 Hz); or (3) use of somewhat more powerful data logger such as the CR23X (CSI) as its cost is less than that of two CR10X and its processing speed is significantly higher.

2.5. Site Description, Instrumentation, and Data

[20] A summary of the main characteristics of the field campaigns is given in Table 2. Six different canopies were analyzed: grass closely meeting the reference crop definition [*Allen et al.*, 1998], wheat, grapevines, rangeland grass and nectarine and olive orchards. Details about the campaigns conducted over grass, wheat and grapevines and data processing can be found in *Snyder et al.* [1996], *Spano et al.* [1997, 2000], and *Castellví* [2004], and for the olive orchard in *Castellví and Martínez-Cob* [2005].

[21] Three experiments over grass (0.1 m high) were carried out at the Campbell Tract Experimental Farm (University of California at Davis) during different years. An omnidimensional sonic anemometer was set at 0.6 m above the ground level during days of year 86, 87, and 88 in 1994 and at 0.7 m during days of year 213 and 214 in 1995. Air temperature traces were recorded at heights of 0.6, 0.9, and 1.2 m in year 1994 and at 0.7, 1.0, and 1.3 m in year 1995. For these two campaigns, measurements were taken under unstable conditions. A three dimensional sonic

anemometer, was set at 1.5 m from days 222 to 234 in 2001. The grass plot was surrounded by short irrigated crops in the main upwind direction and bare soil. Because the surface roughness, within several hundred meters, was similar, it is realistic to assume that the wind profile was not disturbed by the transition. Foot print analysis was carried out according to *Kormann and Meixner* [2001]. The cumulative mean upwind foot print determined under unstable conditions was 89% for year 2001 at 1.5 m, 81% for 1994 at 1.2 m, and 0.80% for 1995 at 1.3 m. However, under stable conditions only 36% was accounted at 1.5 m.

[22] The wheat experiment (0.7 m high) was conducted during days of year 148 and 149 in 1994 at Davis (California). The measurements were made during daylight hours. The experiment conducted over grapevines having 2.0 m height, 60% ground cover and separation between trunks of 1.5 m between plants and 2.7 m in the inter-row with a mean free space of 1.8 m. The experiment was conducted during daylight hours for days of year 226 and 227 in 1995 at the Oakville Field Station in Napa Valley (California). The experiment conducted over olive orchard (3.4 m high, 50% ground cover, 3 m separation between trunks with an inter-row of 6 m wide) occurred in days of year 106 to 208 in 1995 within the Ebro river basin (NE of Spain). The temperature structure functions of order 2, 3 and 5, equation (A1), were recorded in a data logger (CR10X, CSI) at two time lags, 0.25 s and 0.75 s. The rangeland grass experiment, with 0.25 m for the mean vegetation height, is fully described by *Baldocchi et al.* [2004]. Briefly, the site is a grazed grassland opening in a region of oak/grass woodland. The site is situated in undulating topography among the oak/grass savannah biome of eastern California in the foothills of the Sierra Nevada Mountains. The main grass and herb species include bromus, frescue, oat, medusa head and rose clover. The data was recorded from days 135 to 287 in year 2002. Numerical footprint calculations performed with a Lagrangian footprint model [*Baldocchi*, 1997] indicate that the fetch was well within the flux footprint during near neutral and unstable thermal stratification and the measurements did not sense the trees and dead grass during the summer. The nectarine orchard experiment was conducted from days 197 to 204 in year 1989 at Atalia (Portugal). The average tree height was 3.2 m, the ground cover was approximately 85% and separation between trunks was; 3.5 m between trees and 5 m in the inter-row with a mean free space of 1.5 m.

2.6. Canopy Parameters

[23] Because the roughness depth and zero plane displacement are highly dependent on the canopy morphology and its capability to absorb momentum, determination of these parameters requires knowledge of the wind and temperature profiles. Then, they had to be estimated. This was done through the main canopy characteristic distances; the canopy height, h, and the mean spacing of roughness elements, D.

2.6.1. Zero Plane Displacement

[24] It can be estimated as $d \approx 2/3h$ [*Brutsaert*, 1982] for homogeneous canopies like grass, rangeland grass and wheat. For grapevines and nectarine orchard it was also roughly estimated as 2/3h because in the mean stream-wise direction the canopy was dense and overlap through close to the ground and the mean inter-row space was moderate. For the olive orchard, the zero plane displacement was neglected because the canopy was open with no understory and the crown was not dense [*Brutsaert*, 1982].

2.6.2. Roughness Sublayer Depth

[25] It can be estimated as $z^* \approx a\ h$ for homogeneous canopies, where a is estimated between 2 and 3 for tall canopies [*Kaimal and Finnigan*, 1994; *Shaw*, 2002]. In general, *Brutsaert* [1982] reports a wider range, with a from 1.5 to 3.5 and some studies used the approach, $z^* \approx h + 2(h - d)$ [*Chen et al.*, 1997a; *Sellers et al.*, 1986] which falls in a lower range. For sparse tall canopies, z^* is estimated as, $z^* \approx aD + d$ [*Garrat*, 1980], where D is the mean spacing of roughness elements and $a \approx 3$ to 4.6 is a coefficient where the higher values for a within this range are observed under near-neutral stability conditions. For crops planted in rows, *Cellier* [1986] suggested D as the inter-row space with, a, a coefficient slightly higher than 3. *Cellier and Brunet* [1992] reported $a = 3.1$ for sugar cane crop and $a = 4.2$ for maize.

[26] Over grass and rangeland grass, data were collected well above the roughness sublayer and z^* was only estimated for the other canopies. For wheat, measurements were made under unstable conditions with wind speeds mostly lower than 2.5 m s^{-1} at z = 2 m. Then, z^* was estimated as $z^* \approx h + 2(h - d) \approx 1.2$ m. For grapevines, the roughness depth was assumed to be, $z^* = 5.5$ m, which is in between three times the mean space between canopies along the inter-row and three times the canopy height. For the nectarine orchard z^* was estimated as, $z^* = 9.5$ m (about 3 times h) because z^* appeared too short if it is estimated as three to four times D. For the olives orchard, the coefficient $a = 3.5$ was chosen because the area is windy and therefore turbulence was mostly mechanically driven. The roughness depth was estimated as $z^* \approx 12$ m, which is about 3.5 times the distance between trunks (3.5 m).

2.7. Data Processing

2.7.1. Ramp Parameters

[27] Determination of parameter γ in equation (A5) requires high-frequency raw data and post processing. *Chen et al.* [1997b] found that parameter γ is rather robust and constant for practical purposes (Table A1). Following Table A1, γ was set to 1.1 for the low canopies (grass, rangeland grass, wheat and grapevines) and to 1.0 for nectarine and olive orchards. In general, the best time lags to solve equation (A5) were $r_x = 0.2$ s and 0.3 s, for the low canopies and $r_x = 0.5$ s and 0.75 s for the nectarine and olive orchards, respectively.

[28] Under near neutral conditions, the sign of the ramp may not correspond with the measured sensible heat flux. The number of half-hour sample failures obtained for all measurement heights were 64 over grass, 1027 over rangeland grass, 22 over grapevines, 25 over nectarines, and 259 over olives. The failures were found within the following ranges of stability parameter and sensible heat flux (W m^{-2}): $(-0.15 < \zeta < 0.01)$ and $(-18 < H < 7.5)$ for grass; $(-0.02 < \zeta < 0.01)$ and $(-9.0 < H < 9.0)$ for rangeland grass; $(-0.05 < \zeta < 0.01)$ and $(-8.1 < H < 12.3)$ for nectarines; and $(-0.03 < \zeta < 0.02)$ and $(-21.1 < H < 10.5)$ for olives. The number of data analyzed are listed in Table 2 and data within the aforementioned ranges were not included.

Table 3. Performance of Equation (8) for Estimation of Friction Velocity[a]

	Simple Linear Regression			Error Statistics	
Level, m	b	a	R^2	RMSE	UE
		Grass (0.1 m Tall)			
0.6^u	−0.01	1.09	0.72	0.03	75
0.7^u	0.00	1.00	0.90	0.01	82
0.9^u	0.01	1.01	0.89	0.03	66
1.0^u	0.04	0.94	0.91	0.01	46
1.2^u	−0.03	1.29	0.58	0.05	59
1.3^u	0.00	1.19	0.77	0.03	54
1.5^u	−0.03	1.13	0.91	0.02	82
All levels^u	0.00	1.07	0.85	0.02	59
1.5^s	0.02	1.03	0.82	0.04	46
		Rangeland Grass (0.25 m Tall)			
2.0^u	0.01	1.13	0.96	0.02	53
2.0^s	0.01	0.91	0.81	0.02	80
		Wheat (0.7 m Tall)			
0.7^u	**0.00**	**1.12**	**0.87**	**0.04**	**26**
1.0^u	**0.00**	**1.02**	**0.89**	**0.02**	**54**
1.3^u	**0.01**	**0.93**	**0.88**	**0.01**	**91**
All levels^u	**0.03**	**0.90**	**0.76**	**0.02**	**86**
1.3^u	**0.01**	**0.73**	**0.88**	**0.05**	**3**
		Grape Vineyard (2.0 m Tall)			
2.0^u	**0.00**	**1.17**	**0.98**	**0.08**	**8**
2.3^u	**0.01**	**1.14**	**0.99**	**0.08**	**20**
2.6^u	**0.01**	**1.11**	**0.98**	**0.07**	**34**
2.9^u	**0.02**	**1.11**	**0.98**	**0.07**	**18**
All levels^u	**0.01**	**1.13**	**0.98**	**0.08**	**19**
		Olive Orchard (3.4 m Tall)			
3.5^u	**0.01**	**0.90**	**0.96**	**0.05**	**0.**
5.1^u	**0.00**	**1.02**	**0.96**	**0.03**	**0.**
All levels^u	**0.00**	**0.91**	**0.96**	**0.05**	**0.**
3.5^s	**0.00**	**0.92**	**0.96**	**0.04**	**0.**
5.1^s	**0.00**	**1.05**	**0.95**	**0.03**	**0.**
All levels^s	**0.00**	**1.03**	**0.96**	**0.04**	**0.**

[a]The parameters are a, regression slope; b (m s^{-1}), intercept of regression (the measured friction velocity was the independent variable); R^2, coefficient of determination; RMSE (m s^{-1}), root-mean-square error; UE, unsystematic percentage of the mean square error. Superscript indexes in parentheses *u* and *s* denote unstable and stable surface layer atmospheric conditions, respectively. Estimates made in the roughness sublayer in bold.

2.7.2. Temperature Structure Function Parameter

[29] The second-order structure function was employed to determine the temperature structure function parameter as $D^2_{(x)} = C_{tt}x^{2/3}$, where $D^2_{(x)}$ and x denotes the second-order structure function and the spatial separation between the two measurements of temperature, respectively [*Stull*, 1991]. The Taylor hypothesis of frozen turbulence can be used to convert time series into spatial series as $S^2_{(r)} = C_{tt}(\bar{u}r)^{2/3}$, where $S^2_{(r)}$ and r were defined in (A1) (for n = 2) and $\bar{u}$ denotes the mean wind speed along the flow direction. The Taylor's frozen hypothesis was used to convert time lags into stream-wise distances using horizontal wind speeds measured with a 3-D sonic anemometer during experiments over grass in year 2001 and the rangeland grass. When 3-D sonic measurements were unavailable, cup anemometer measurements were corrected at different levels using the wind profile law (experiments over grass in 1994 and 1995).

2.7.3. Stability Parameter and Sensible Heat Flux

[30] Over the grass experiments, where the Obukhov length was unavailable, iteration based on the wind profile law [*Brutsaert*, 1982] was used to solve for convergence of the conjunction of friction velocity, stability parameter, and sensible heat flux by starting the iteration process assuming neutral conditions. A description is given by *Castellví et al.* [2002] and *Castellví* [2004]. For the experiments over grass in year 2001 and rangeland grass the measured air temperature, friction velocity and sensible heat flux were used to determine the stability parameter. For the olive orchard, horizontal wind speed was available at a single level close to the canopy top. Friction velocity was estimated using the measured horizontal wind speed at the canopy top [*Kaimal and Finnigan*, 1994]. Simulating annealing procedure in conjunction with the Metropolis criteria was used for stability parameter and sensible heat flux optimization. Details about the procedure are given by *Castellví and Martínez-Cob* [2005]. For the nectarine orchard experiment, the friction velocity, stability parameter, and horizontal wind speed above the canopy were unavailable. Under unstable atmospheric conditions, the scale $\lambda^*_{(\zeta)}$ was used (Appendix B) to compute $u_* \approx z/[\tau\lambda^*_{(\zeta)}] \approx z/[\tau 0.75^3]$. The friction velocity was estimated using the relationship $u_* \approx [\langle w'^2\rangle/1.7]^{0.5}$ where $\langle w'^2\rangle$ is the variance of the vertical wind velocity that was recorded each half hour [*Stull*, 1991]. Under stable atmospheric conditions, friction velocity was estimated using only $u_* \approx [\langle w'^2\rangle/1.7]^{0.5}$ because the scale $\lambda^*_{(\zeta)}$ was uncertain. The stability parameter was obtained from the Obukhov length using the corresponding estimated u_* and the measured sensible heat flux.

2.8. Procedure to Analyze Estimates Performance

[31] The performance of equation (8) for estimating friction velocity and the new and existing equations for estimating sensible heat flux was analyzed in terms of linear regression analysis (the measured values were taken as the independent variable), coefficient of determination, R^2, and the root mean square error, RMSE. However, the RMSE values were also analyzed in terms of systematic, RMSEs, and unsystematic, RMSEu, parts (see Table 1), where $RMSE^2 = RMSEu^2 + RMSEs^2$ [*Willmott*, 1982]. The portion of the systematic errors presumably contained in the model, SE (expressed in %), can be described by $SE = 100\ RMSEs^2/RMSE^2$. When SE is high, it is possible to dampen a new parameterization of the model without making significant changes in model's structure. Therefore the expression UE = 100 − SE can be interpreted as a measure of potential accuracy improvement.

3. Results

3.1. Friction Velocity

[32] Table 3 lists the statistics obtained corresponding to the performance of equation (8) in estimating the friction velocity except for the nectarine orchard because direct measurement was unavailable. In general, whatever the measurement level and stability conditions, including homogeneous and heterogeneous canopies, the intercepts were negligible, R^2 values were high, and the RMSE values were small. The relatively high UE percentages observed in

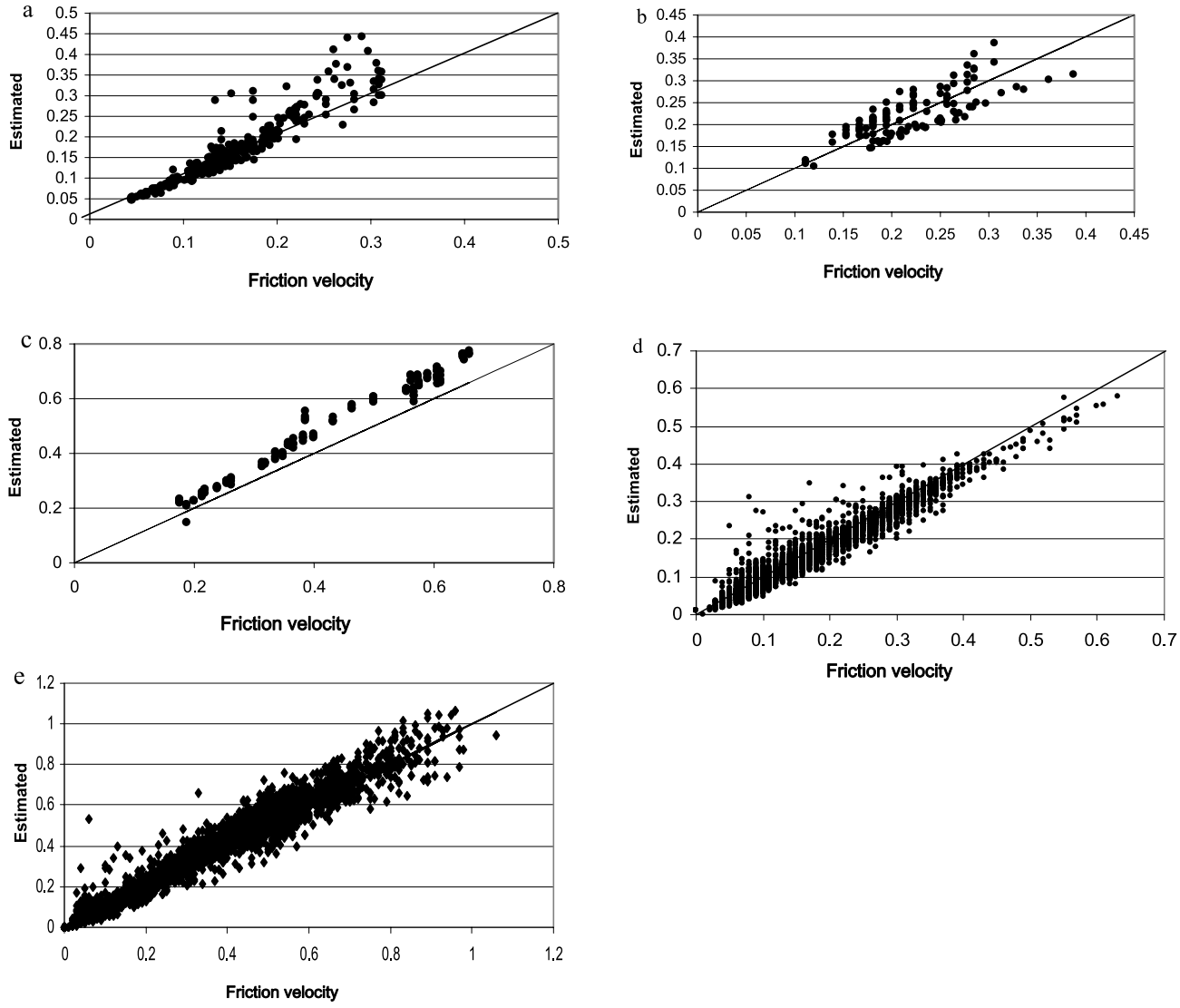

Figure 1. Performance of equation (8) estimating friction velocity (m s^{-1}) over (a) grass, (b) wheat, (c) grapevines, (d) rangeland grass, and (e) olive orchard for all measurements heights. The 1:1 line is introduced for comparison.

Table 3 are as a consequence of the small RMSE values. Figure 1 shows friction velocity estimates for the entire data set including the six canopies. It is shown that equation (8) was robust and accurate.

3.1.1. Measurements Taken in the Inertial Sublayer

[33] In the experiments over grass and rangeland grass, performance was generally excellent regardless of the stability conditions. Under unstable conditions, measurements collected up to 1 m revealed a consistent overestimation on the order of 15% Except for the 1.5 m height over grass, the UE $\approx$ 55% were reasonably good. A better selection of parameters d and γ would likely provide slopes closer to one. Nevertheless, the RMSE were small. Over rangeland grass, equation (8) was able to mostly capture the full measured friction velocity variability. Over grass, the overestimation may be attributed to a lack of fetch. Entrainment of air from above the adjusted surface layer likely contaminated the air temperature traces, which may explains the substantial reduction in R^2 relative to the 0.7, 0.9, and 1.0 m measurements. The 0.6 m level also performed poorly relative to the 0.7, 0.9, and 1.0 m heights. It was probably too close to the surface and it required a higher measurement frequency. Under stable conditions, the estimates were good although equation (8) performed better for rangeland grass than for grass. It was likely due to differences in fetch.

3.1.2. Measurements Taken in the Roughness Sublayer

[34] Table 3 shows that over wheat, the performance was good. For the upper level (1.3 m), the statistics listed in Table 3 were determined assuming that measurements occurred within the roughness and inertial sublayers. The results were better when it was assumed that the data were collected in the roughness rather than the inertial sublayer For the inertial sublayer, there was an underestimation up to 25% and the UE = 3% was small, indicating that most RMSE was systematic. This observation suggests a deeper roughness sublayer. Lower accuracy was observed for measurements at the canopy top, and a higher measurement frequency would likely improve accuracy. For all measurement levels, equation (8) had an underestimation

Table 4. Estimates of H from Equation (6), (13), (14), (18), (19), (20), (21), (22), (23), and (24) Using Data Collected Within the Inertial Sublayer[a]

	Equation (6)					Equation (13)					Equation (14)					Equation (21)					Equation (22)				
Level	a	b	R^2	RMSE	UE	a	b	R^2	RMSE	UE	a	b	R^2	RMSE	UE	a	b	R^2	RMSE	UE	a	b	R^2	RMSE	UE
Grass (0.1 m Tall)																									
0.6^u	0.96	0.2	0.97	5.3	92	1.07	−8.3	0.81	14.7	89	1.09	−8.2	0.80	14.8	91	1.10	4.7	0.85	11.6	93	1.15	4.1	0.85	11.8	76
0.7^u	0.97	−1.1	0.96	3.1	90	1.08	−4.8	0.84	3.8	48	1.10	−4.3	0.85	3.5	57	1.00	−0.6	0.98	0.3	88	0.99	−1.6	0.98	1.3	12
0.9^u	1.00	0.5	0.98	4.9	92	1.07	−8.1	0.88	11.8	86	1.09	−7.9	0.89	11.6	89	1.05	2.5	0.85	13.1	98	1.09	2.0	0.87	14.1	88
1.0^u	0.98	4.3	0.93	4.2	89	1.27	−11.9	0.83	5.5	19	1.29	−10.1	0.83	5.3	24	1.03	−0.4	0.50	4.4	95	1.01	−1.4	0.49	4.1	88
1.2^u	1.00	7.0	0.95	7.3	94	1.09	−11.1	0.85	15.7	84	1.11	−11.5	0.85	15.5	86	0.95	0.5	0.80	15.1	94	1.00	0.0	0.80	15.7	99
1.3^u	1.11	10.1	0.88	4.2	79	1.36	−13.2	0.76	6.2	38	1.39	−12.5	0.77	6.8	24	0.97	−3.5	0.82	4.5	95	0.85	−4.5	0.82	4.4	94
1.5^u	0.97	5.7	0.83	12.9	87	1.01	18.2	0.53	19.3	79	1.04	17.2	0.51	19.9	78	0.86	−11.9	0.66	15.2	85	0.85	−10.5	0.65	17.3	77
All levels^u	0.99	2.8	0.90	8.1	86	0.81	8.2	0.69	16.4	79	0.80	7.7	0.68	16.8	79	0.86	−5.5	0.77	14.7	87	1.01	−6.5	0.78	13.0	79
1.5^s	1.00	−7.7	0.85	3.9	85	0.92	3.2	0.46	9.5	71	1.14	5.2	0.42	13.2	70	0.70	−21.5	0.12	23.0	53	0.68	−25.8	0.00	29.5	31
Rangeland Grass (0.25 m Tall)																									
2.0^u	1.02	−10.1	0.95	26.1	96	0.98	2.3	0.95	33.6	95	0.87	1.1	0.92	38.2	53	0.87	−15.5	0.93	76.8	41	1.10	−5.1	0.93	49.5	39
2.0^s	0.56	−20.1	0.29	11.3	84	0.44	−17.5	0.22	13.1	87	0.47	−20.3	0.20	15.1	88	0.36	−9.5	0.12	14.1	97	0.30	−57.5	0.00	73.3	99

	Equation (20)					Equation (18)					Equation (19)					Equation (23)					Equation (24)				
Level	a	b	R^2	RMSE	UE	a	b	R^2	RMSE	UE	a	b	R^2	RMSE	UE	a	b	R^2	RMSE	UE	a	b	R^2	RMSE	UE
Grass (0.1 m Tall)																									
0.6^u	0.98	−8.6	0.81	15.3	78	0.93	−8.1	0.86	11.4	81	0.84	−7.2	0.86	11.7	38	1.10	5.5	0.78	23.4	23	0.87	7.2	0.73	21.9	44
0.7^u	1.04	−5.5	0.92	5.2	91	1.10	3.5	0.83	2.6	93	0.95	1.8	0.83	1.4	37	1.00	9.3	0.83	7.5	13	0.87	4.5	0.92	5.9	7
0.9^u	1.00	0.5	0.83	12.7	99	0.85	−7.9	0.90	8.3	81	0.90	−8.8	0.90	10.8	72	0.99	4.0	0.75	20.5	37	0.87	4.1	0.72	17.8	56
1.0^u	1.07	1.0	0.88	9.2	95	0.94	−1.2	0.83	2.3	95	0.96	−2.6	0.80	5.2	77	1.07	8.5	0.91	4.2	27	1.02	3.4	0.48	6.8	70
1.2^u	1.03	−0.2	0.78	15.7	99	0.91	−8.2	0.90	8.5	68	1.00	−10.6	0.90	15.6	37	0.95	3.3	0.79	18.1	46	0.81	2.1	0.73	17.5	55
1.3^u	1.17	11.2	0.77	7.7	21	0.86	−10.5	0.67	4.6	67	0.89	−14.4	0.59	13.8	84	0.86	4.5	0.82	4.2	58	0.85	−1.4	0.77	5.9	61
1.5^u	1.10	12.2	0.64	15.8	27	0.90	−16.4	0.75	15.0	62	0.86	−13.5	0.69	13.2	84	0.86	−32.0	0.04	39.5	82	1.14	−12.8	0.72	13.2	84
All levels^u	1.01	4.6	0.72	16.4	85	1.02	−8.9	0.80	13.4	83	0.95	−8.6	0.80	11.8	73	0.83	−8.0	0.35	29.5	75	0.90	−3.7	0.77	12.3	87
Rangeland Grass (0.25 m Tall)																									
2.0^u	1.02	12.1	0.95	31.8	91	1.01	4.0	0.96	26.9	98	1.07	7.6	0.96	21.2	89	0.62	−1.1	0.88	90.7	23	1.37	17	0.93	131.2	14

[a]Regression slope, a; Intercept of regression, b (W m^{-2}); Coefficient of determination, R^2; root-mean-square error, RMSE (W m^{-2}); Unsystematic percentage of RMSE, UE. The measured H was the independent variable. Superscript index *u* and *s* denote unstable and stable surface layer atmospheric conditions, respectively.

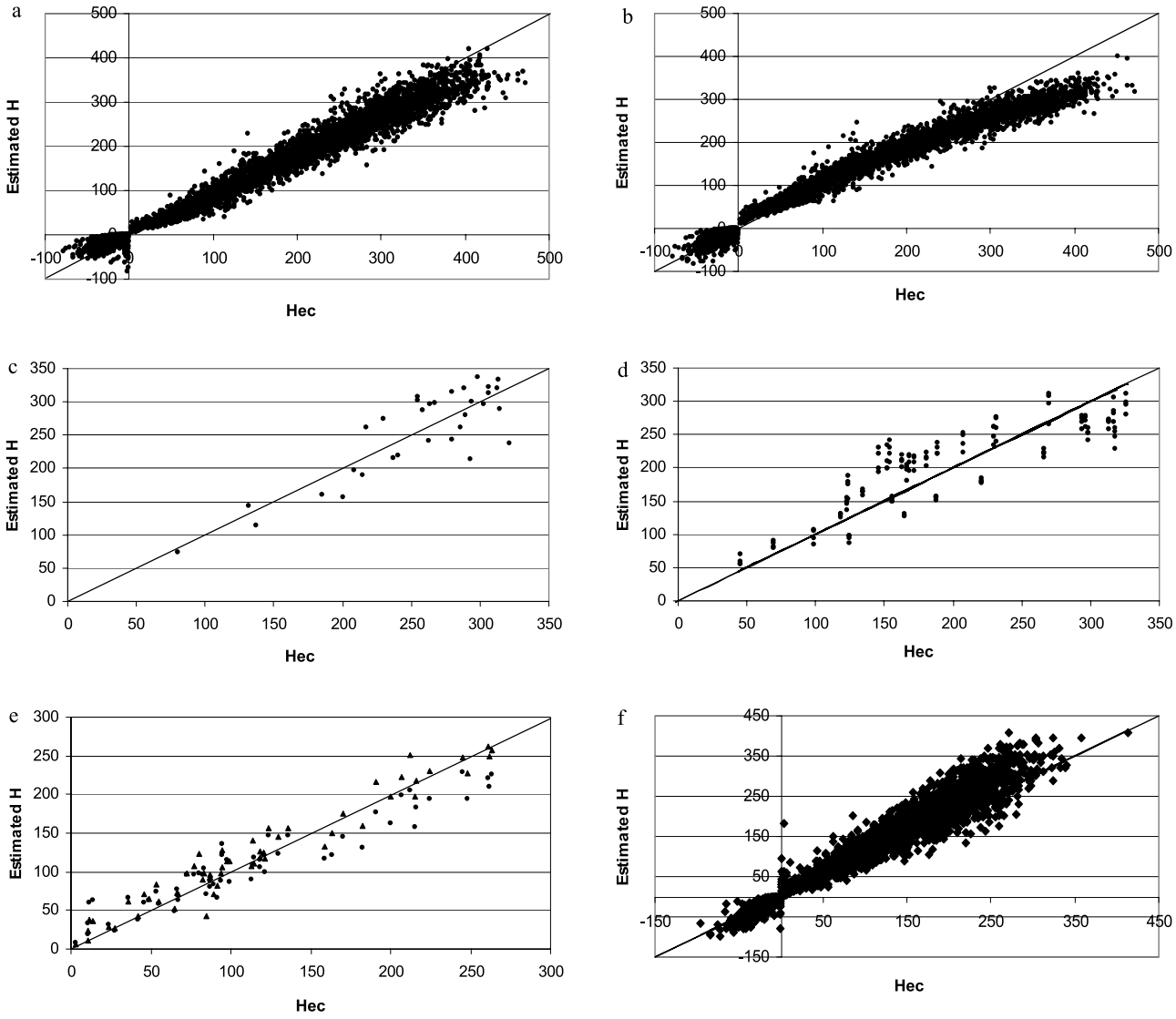

Figure 2. Estimated versus measured with the eddy covariance, Hec (in W m^{-2}), sensible heat flux over (a) rangeland grass with equation (13), (b) rangeland grass with equation (14), (c) wheat, (d) grapevines using equation (19), (*e*) nectarine orchard using equations (19) (circles) and (20) (triangles), and (f) olive orchard using equation (17) for all measurements heights. The 1:1 line is introduced for comparison.

of 10% that could be corrected (slope of one) by increasing the roughness sublayer depth to 2.85 times the canopy height.

[35] For the grapevine experiment, equation (8) generally overestimated by around 13% at all measurement levels. Performance was excellent for the olive orchard regardless of the stability conditions and measurement level, although the highest level was slightly more accurate. For these two canopies, the low UE values obtained for all levels indicate that an accurate selection for parameters, d, z* and γ would substantially improve the estimates. These parameters affect the slope value and induce systematic error.

3.2. Sensible Heat Flux

3.2.1. Measurements Taken in the Inertial Sublayer

[36] Table 4 lists the statistics for all heights to show the performance of equations (6), (13), (14), (21), (22) and of their respective free convection limit approaches, equations (20), (18), (19), (23) and (24) for the experiments over grasses. As an example, Figure 2 shows H values obtained with equations (13) and (14) over rangeland grass (Figures 2a and 2b). Figures showing the performance of equation (6) over grass are published by *Castellví* [2004]. It is shown that estimates were accurate.

3.2.1.1. Unstable Conditions

[37] For the grass experiments, all 10 equations performed well. In general, the slope and R^2 values were close to one, and the intercept and RMSE values were small. For equations requiring air temperature and wind speed measurements, the maximum RMSE value obtained was RMSE = 19.9 W m^{-2} using equation (14) at the 1.5 m level. For the free convection limit approaches, the maximum RMSE value obtained was RMSE = 39.5 W m^{-2}

Table 5. Estimates of H From Equations (6), (17), (20), and (19) Using Data Collected Within the Roughness Sublayer[a]

	Equation (6)					Equation (17)					Equation (20)					Equation (19)				
Level	a	b	R^2	RMSE	UE	a	b	R^2	RMSE	UE	a	b	R^2	RMSE	UE	a	b	R^2	RMSE	UE
Wheat (0.7 m Tall)																				
0.7^u	1.07	12.1	0.74	58.3	99	1.05	−0.7	0.79	42.1	87	0.94	15.7	0.66	47.3	99	1.08	−0.8	0.77	45.1	80
1.0^u	1.00	3.5	0.77	45.7	89	1.04	−4.4	0.79	45.5	83	0.92	5.5	0.73	41.7	86	1.08	3.0	0.77	47.5	74
1.3^u	0.99	2.5	0.76	42.4	87	0.97	1.6	0.82	31.0	98	0.90	−2.4	0.78	44.4	81	1.00	−2.0	0.80	34.6	99
All levels^u	1.02	−2.0	0.70	49.4	99	1.04	−11.0	0.79	39.2	99	0.96	−4.5	0.70	44.4	89	1.09	−10.5	0.77	42.5	88
1.3^u	**0.69**	**−0.5**	**0.76**	**89.1**	**14**	**0.74**	**−3.0**	**0.82**	**91.6**	**4**	**0.67**	**−1.7**	**0.78**	**90.4**	**8**	**0.63**	**−1.3**	**0.80**	**114.6**	**4**
Grape Vineyard (2.0 m Tall)																				
2.0^u	1.06	6.5	0.93	29.0	56	1.15	45.2	0.91	80.9	11	0.94	57.4	0.90	52.4	20	0.93	106.2	0.60	108.4	27
2.3^u	1.09	−5.1	0.93	27.0	71	1.11	30.8	0.88	62.6	25	1.01	41.4	0.88	52.7	27	1.00	93.4	0.60	113.2	29
2.6^u	1.02	−4.4	0.94	21.0	98	1.05	27.1	0.91	46.2	31	0.98	39.3	0.90	42.9	31	0.96	92.1	0.61	102.8	32
2.9^u	1.07	−8.4	0.94	20.6	85	1.06	33.0	0.90	53.5	27	1.02	42.2	0.90	53.7	23	0.97	101.9	0.60	114.2	28
All levels^u	1.06	−2.7	0.93	24.7	73	1.09	34.2	0.87	62.2	21	0.99	45.0	0.89	50.6	25	0.97	98.3	0.60	109.7	29
Nectarine Orchard (3.2 m Tall)																				
3.2^u	–	–	–	–	–	–	–	–	–	–	0.94	−10.2	0.93	18.3	21	0.75	23.5	0.85	25.5	47
3.2^{u1}	0.93	−10.2	0.91	22.0	23	0.86	20.3	0.71	30.9	87	–	–	–	–	–	–	–	–	–	–
3.2^{u2}	0.97	16.8	0.93	25.6	45	0.85	31.4	0.85	22.0	62	–	–	–	–	–	–	–	–	–	–
3.2^{s2}	1.00	−13.4	0.30	21.3	60	1.03	−17.6	0.14	28.2	78	–	–	–	–	–	–	–	–	–	–
Olive orchard (3.4 m Tall)																				
3.5^u	1.07	13.2	0.93	35.4	62	1.32	8.5	0.89	41.5	27	1.03	10.8	0.85	39.8	82	1.14	8.0	0.85	50.6	79
5.1^u	0.91	5.6	0.93	23.4	91	1.11	4.4	0.90	30.1	48	0.92	3.0	0.87	31.0	86	1.06	1.6	0.88	34.3	88
All levels^u	1.01	3.2	0.94	28.1	89	1.18	4.0	0.90	32.7	41	0.99	3.5	0.87	34.2	97	1.08	3.5	0.87	40.3	82
3.5^s	1.15	1.7	0.98	19.5	13	1.25	−0.5	0.77	12.4	65	–	–	–	–	–	–	–	–	–	–
5.1^s	1.09	0.7	0.83	7.6	99	1.13	0.4	0.78	8.3	77	–	–	–	–	–	–	–	–	–	–
All levels^s	1.11	0.5	0.87	10.6	89	1.19	0.0	0.78	10.3	72	–	–	–	–	–	–	–	–	–	–

[a]Regression slope, a; intercept of regression, b (W m^{-2}); coefficient of determination, R^2; root-mean-square error, RMSE (W m^{-2}); unsystematic percentage of RMSE, UE. The measured H was the independent variable. Superscript index *u* and *s* denote unstable and stable surface layer atmospheric conditions, respectively. Estimates assuming the level in the inertial sublayer in bold. Friction velocity determined as (1) $u_* = z/[0.42\tau]$ and (2) $u_* = [\langle w'^2 \rangle/1.7]^{0.5}$.

using equation (21) at the 1.5 m level. All the other cases had RMSE values less than 25 W m^{-2}, which is the expected error for an eddy covariance system [*Paw U et al.*, 1995]. Most UE percentages were high, indicating little room for improvement.

[38] For the 1.5 m level, equation (23) was not able to capture the measured H variability as well as the other equations, which require only temperature data. This was likely a consequence that the free convection limit for (21) holds for a narrower range of the stability parameter ($\zeta < -0.14$) than it does for the other equations. For this level, equation (23) performed poorly especially in the range $-0.28 \leq \zeta \leq 0$. Regardless of the equation being based on similarity principles or not, the measured H variability tended to be better captured for the lower than for the higher levels, thus suggesting lack of fetch. For the same plot, this trend was also found in *Snyder et al.* [1996] for equation (1) when calibrating the parameter α.

[39] For rangeland grass, the best performance for equations requiring air temperature and wind speed measurements was obtained using equation (6). The other SR-based equations, however, also performed well. For equations depending on the temperature parameter structure function, the performance obtained from equation (13) was better than for (21). For equations depending on the temperature standard deviation, the performance obtained from equation (14) was slightly better than for (22).

[40] For the free convection limit approaches, equations (20), (18) and (19) were comparable. Their performance was excellent and comparable to their respective expressions requiring wind speed measurements as input. The intercept and R^2 value for equations (23) and (24) were good, but the slopes departed considerably from unity. The RMSE values obtained for (23) and (24) were high, but the low UE percentages obtained indicate a potential for improvement. Previous site-specific calibration of their corresponding similarity relationships would substantially reduce the RMSE. This issue suggest that for this experiment, the new derived equations were less sensitive to the site performance of $g_1(\zeta)$ and $g_2(\zeta)$ than those equations exclusively based on similarity. Equation (13) depends of the power $-1/6$ on $g_1(\zeta)$, but equation (21) on the power $-3/4$. Equation (14) depends of the power $-1/3$ on $g_2(\zeta)$, whereas equation (22) on the power $-2/3$.

3.2.1.2. Stable Conditions

[41] For the grass experiment, equations (6), (13) and (14) performed well. The RMSE values were small indicating that these three equations, especially equation (6), showed similar accuracy to the eddy covariance. The UE percentages obtained were relatively high because the RMSE were small. For rangeland grass, all three equations gave similar results but poor accuracy. The slopes and intercepts were around 0.5 and 20 W m^{-2}, respectively, R^2 values were around 0.25, and most of the RMSE (up to 85%) was unsystematic indicating the poor potential for improvement.

[42] The flux variance method using equations (21) and (22) showed poor performance for both grass or rangeland

grass. Fetch for the rangeland experiment was adequate, but the performance from all the equations was worse than for the grass experiment. For rangeland grass, the corresponding relationships in equation (14), $g_1(\zeta)$ and $g_2(\zeta)$, did not hold under stable conditions. This and the poor performance obtained using equations (6), (13) and (14) might have resulted as a consequence of cool air drainage during nighttime.

3.2.2. Measurements Taken in the Roughness Sublayer

[43] Table 5 lists the statistics corresponding to equations (6) and (17) and for their respective free convection limit approaches, equations (20) and (19), for each measurement level and for the whole data set from experiments over wheat, grapevines, and nectarine and olive orchards. H values obtained with equation (19) are shown for all the measurement heights over wheat (Figure 2c) and grapevines (Figure 2d). Equations (19) and (20) show H values measured over nectarine orchard (Figure 2e) and equation (17) illustrates the H measurements over the olive orchard (Figure 2f). Figures showing the performance of equation (6) for wheat and grapevines are published by *Castellví* [2004] and the estimates from equations (6), (20) and (22) over the olive orchard are provided by *Castellví and Martínez-Cob* [2005]. It is shown that estimations were good.

3.2.2.1. Wheat Experiment

[44] As observed for the friction velocity estimates, H estimates were better at the 1.3 m level when it was assumed that the measurement level was located in the roughness sublayer. When all equations were applied in the inertial sublayer, most of the RMSE portion was systematic, the UE ranged from 4% to 14%. When all equations were applied assuming data collection within the roughness sublayer, the slopes were in the range 0.9 to 1.08 and the intercepts were near zero regardless of the measurement height. The UE percentages were high because the equations were not able to fully capture the measured sensible heat flux variability (R^2 values ranged from 0.66 to 0.82). The RMSE values, however, were reasonably good in all cases and equation (17) had slightly better performance than (6). This was also observed for their free convection limit approaches using equations (19) and (20), respectively.

3.2.2.2. Grapevines Experiment

[45] Equation (6) had excellent performance for all levels. The slopes and R^2 values were close to unity and the intercept and RMSE values were small. Equation (17) gave biased results for all levels, but it was able to capture most of the measured H variability. The performance improved with the measurement height and the low UE values obtained indicate that the bias produced high systematic error.

[46] The corresponding free convection limits approaches for equation (6) and (17), equation (20) and (19), respectively, had slopes close to 1.0 for all the levels but resulted in more bias. Equations (20) and (19) had small UE percentages indicating that correction of the bias would greatly reduce the RMSE. The assumptions made when using equation (18) may resulted in rather unrealistic H values for this heterogeneous canopy. This may explain the why equation (6) performed better than (17) as did the corresponding free convection limit approaches.

3.2.2.3. Nectarine Orchard Experiment

[47] Under unstable conditions, equation (6) showed excellent performance regardless of the level and method used for estimating the friction velocity. The RMSE values obtained were small. The UE percentages were low and some bias was observed. Equation (6) was more accurate than (17) and it better represented the measured H variability. The RMSE values obtained using equation (17), however, were also good. The performance given by equation (6) was comparable to its free convection limit approach, equation (20). Equation (19), the free corresponding free convection limit approach to equation (17), performed better than (17). This was probably due to inaccuracy in the similarity relationships operating near the canopy top.

[48] Under stable conditions, equations (6) and (17) had reasonably good performance. Sensible heat fluxes were within a narrow range, $-47.3 \leq H \leq 0.0$ W m^{-2}, and most samples fell within the measurement error, which makes interpretation of the statistics listed in Table 5 difficult. Overall, regardless of the measurement level, the method for estimating the friction velocity and stability of the surface layer, equations (6) and (20), which are based on ramp amplitude, performed slightly better than those based on the standard deviation, equations (17) and (19).

3.2.2.4. Olive Orchard Experiment

[49] Regardless of the measurement level or stability conditions, the equations performed well, and the RMSE values were small. The UE percentages for equation (6) were higher than for equation (17), probably because the RMSE were smaller. Equation (6) was more accurate. The same was observed for their free convection limit approaches. All of the equations had near zero intercept values.

3.2.3. Overall Results

[50] All of the equations performed reasonably well for all of the vegetation; however, the equations based on ramp amplitude were generally more accurate. The fact that equations (17) and (19) over wheat and the two orchards (nectarine and olive) showed good performance indicates that equation (16) gave realistic results for homogeneous and some heterogeneous canopies. It did not seem true for heterogeneous canopies, such as grapevines. To test the equation (16) performance over grapevines requires data that were unavailable. Likely, the H estimates would be improved if all canopy and ramp parameters were determined. However, determination of the zero plane displacement, roughness layer depth and parameter γ requires knowledge of the profiles of wind speed and temperature and much higher frequency measurement. It was shown that the SR based equations did in most of the cases a very good performance and that automatically accounted for canopy and ramp parameters changes because as vegetation grows they can be estimated according to the new canopy or plants architecture.

3.2.4. Flux-Variance Method

[51] Although mainly for equation (24), the flux-variance method has also been tested under nonideal field conditions [*Weaver*, 1990; *De Bruin et al.*, 1991; *Katul et al.*, 1995, 1996; *Wesson et al.*, 2001]. Equations (22) and (24) were analyzed for the experiments over wheat and grapevines by *Castellví* [2004] and for the olive orchard by *Castellví and Martínez-Cob* [2005]. The results obtained indicate that new equations (17) and (19), depending on the temperature standard deviation, were comparable or performed better than (22) and (24), respectively. For the olive orchard

experiment, under stable atmospheric conditions, the flux-variance method was not applicable because the similarity relationship, $g_2(\zeta)$, was uncertain [*Castellví and Martínez-Cob*, 2005]. Equation (17), however, performed reasonably well (Table 5) indicating it was robust relative to (22) under conditions unfavorable to meeting similarity requirements. Equation (17) depends on $g_2(\zeta)$ less than (22).

[52] For the nectarine orchard, the H estimates from equations (22) and (24) were often poor for values of H less than 70 W m^{-2}. This indicated that close to the canopy $g_2(\zeta)$ held better when thermal convection becomes important (i.e., turbulence tends to be decoupled from the surface). Equations (17) and (19) were mostly superior to (22) and (24) for H values below 95 W m^{-2}. Under stable atmospheric conditions, equation (22) exhibited poor regression statistics, with slope, intercept and R^2 values of 0.42, −8.6 W m^{-2}, and 0.07, respectively. The RMSE = 32.1 W m^{-2} and UE = 91% indicating that equation (22) was inferior to equation (17).

4. Summary and Concluding Remarks

[53] On the basis of SR analysis and similarity principles, two new equations (13) and (14) for estimating sensible heat flux, using measurements taken in the inertial sublayer were presented. The new equations are based on equation (8) for estimating friction velocity. Equation (8) was combined with three relationships that are valid for estimating the temperature scale (T_*) in the inertial sublayer (equations (9), (11) and (12)) giving equations (13) and (14). Equation (13) depends on the parameter of the temperature structure function and (14) on the standard deviation of temperature. Their respective free convection limits, equations (18) and (19), exhibited a weak dependence on the stability parameter under slightly unstable conditions permitting sensible heat flux estimates from air temperature as the only input under unstable conditions. Equation (14) was modified for operating above but close to the canopy top, equation (17). The free convection limit for (17) also held for slightly unstable conditions, equation (19).

[54] When measuring in the inertial sublayer the new equations generally showed excellent performance under unstable conditions. The results obtained suggest that equations (13) and (14) and their respective free convection limit expressions provide a practical technique to apply the SR analysis. In the roughness sublayer, equations (17) and (19) were robust even when measurements are made over rather heterogeneous nectarine and olive orchards canopies, but biased for a heterogeneous grapevine canopy.

[55] The new equations are less sensitive to similarity functions than are equations (21) and (22), which are exclusively based on similarity principles. This is convenient for two reasons. First, similarity functions may require site-specific adjustment when similarity grounds are not fully met such as when measuring over growing vegetation or close to the canopy. Also, measuring close to the canopy top reduces fetch requirements and the need for tall micrometeorological towers. Second, similarity based equations are sensitive to measurement height above the zero plane displacement, which must be estimated unless wind profile are available.

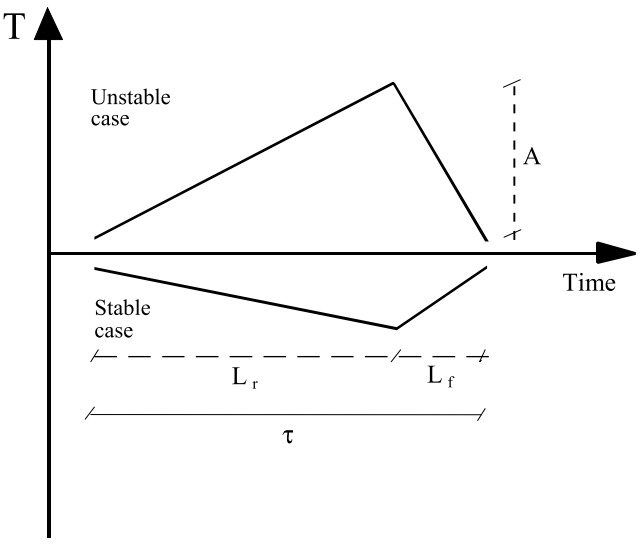

Figure A1. Ramp model with amplitude, A, and duration, τ, assuming a finite microfront duration, L_f. The quiescent time period is neglected.

[56] Under stable conditions, the combined SR similarity equations are superior to the exclusively similarity-based equations (21) and (22). The similarity functions performance, however, still played a key role, which explains why equation (6) showed the best performance. Moreover, equation (6) shows a z* dependence on the power 3/5, while equations (17) and (19) on the powers 1 and $^1/_2$, respectively. Therefore equation (6) is more robust to uncertainties when estimating the roughness depth.

[57] In conclusion, it was shown that the equations obtained as a result of combining SR analysis and similarity principles are more robust than those based solely on similarity either when measuring well above or close to the canopy top and over nonhomogeneous canopies. The SR based equations automatically account for calibration coefficient changes because as vegetation grows they can be estimated according to the new canopy architecture. Equation (6) and its free convection limit generally performed best because (6) is less similarity dependent. Equation (19) appeared attractive for field applications. It performed well and permits affordable battery-powered data loggers to record temperature and compute sensible heat flux on−line.

Appendix A: Ramp Parameters

[58] Structure functions, equation (A1), and the analysis technique, equations (A2) to (A4), from *Van Atta* [1977] were used to determine ramp amplitude, A:

$$S^n_{(r)} = \frac{1}{m-j}\sum_{i=1+j}^{m}\left(T_i - T_{i-j}\right)^n \qquad \text{(A1)}$$

where m is the number of data points in the 30-min interval measured at frequency (f), n is the power of the function, j is a sample lag between data points corresponding to a time lag ($\mathbf{r} = j/f$), and T_i is the ith temperature sample. An

Table A1. Recommended Mean Values for γ, r_x (s) and Sampling Frequencies for Different Canopies[a]

Canopy Height	γ	Hz	r_x
Fir forest, 16.7 m	1.001	5	0.833
Straw mulch, 0.06 m	1.175	11	0.111
Bare soil	1.104	26	0.066

[a]Sampling frequencies are Hz. From *Chen et al.* [1997a].

estimate of the mean value for A is determined by solving equation (A2) for the real roots

$$A^3 + pA + q = 0 \tag{A2}$$

where

$$p = 10S^2_{(r)} - \frac{S^5_{(r)}}{S^3_{(r)}} \tag{A3}$$

and

$$q = 10S^3_{(r)} \tag{A4}$$

According to ramp scheme in Figure A1, the relationship between the inverse ramp frequency ($\tau = L_r + L_f$) and ramp amplitude [*Chen et al.*, 1997a] is

$$\frac{A}{\tau^{1/3}} = -\gamma\left(\frac{S^3_{(r_x)}}{r_x}\right)^{1/3} \tag{A5}$$

where r_x is the time lag r that maximizes $(S^3(r)/r)$ and γ is a parameter that corrects for the difference between $A/\tau^{1/3}$ and $(S^3(r)/r)^{1/3}$ evaluated at r_x. Parameter γ varies by less than 25% with respect to unity, (0.9–1.2) for the range of canopies in Table A1. For bare soil and straw mulch parameter γ mainly varies between (1 and 1.2), while for Douglas fir Forest it mainly varies between (0.9 and 1.1). Mean values for parameters γ and r_x and the suitable

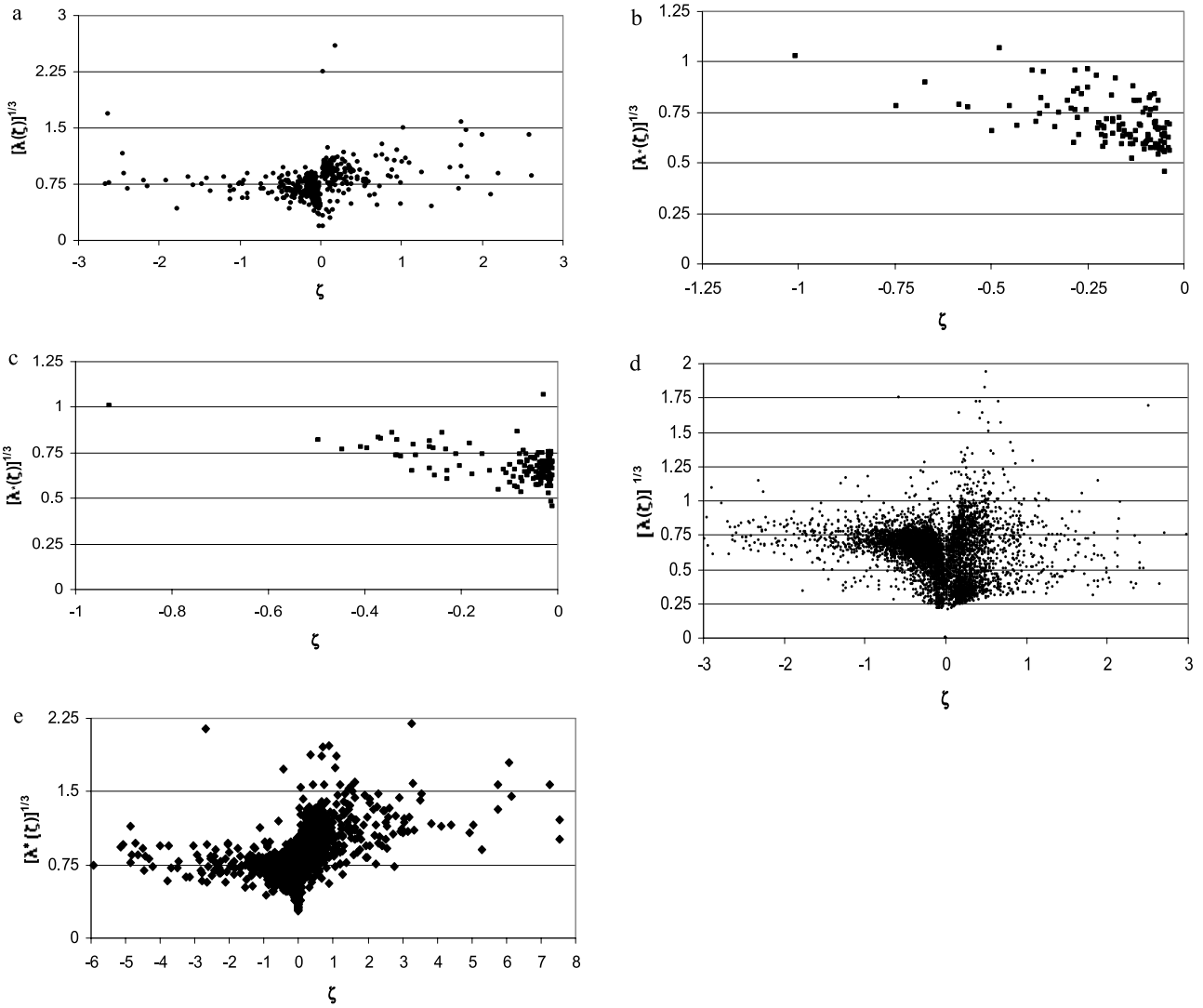

Figure B1. The scales $[\lambda_{(\zeta)}]^{1/3}$ and $[\lambda^*_{(\zeta)}]^{1/3}$ versus the stability parameter for (a) grass, (b) wheat, (c) grapevines, (d) rangeland grass, and (e) olive orchard. All measurements are heights.

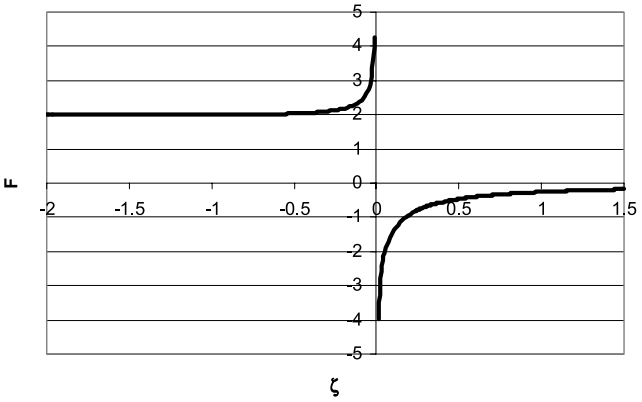

Figure B2. Composed similarity functions, $F_1(\zeta) = \phi_h^{-1/2}(\zeta)\, g_1^{-1/6}(\zeta)/(-\zeta)^{1/3}$ in equation (13), and $F_2(\zeta) = \phi_h^{-1/2}(\zeta)\, g_2^{-1/3}(\zeta)/(-\zeta)^{1/3}$ in equations (14) and (17) versus the stability parameter. Because $F_1(\zeta)$ and $F_2(\zeta)$ are undistinguishable, the function $F = F_1(\zeta)$ is shown.

measurement frequencies, Hz, required for different canopies to solve (A5) (i.e., to capture the appropriate solution to A5 for most samples) are shown in Table A1.

Appendix B: Analyzing the Atmospheric Stability Dependence for Estimating Sensible Heat Flux From Equations (13), (14), and (17)

[59] Combining equations (3) and (4), the following expression for parameter $[\alpha(k\beta)^2]^{1/3}$ is obtained

$$\left[\alpha(k\beta)^2\right]^{1/3} = \begin{cases} \left(\frac{k}{\pi}\right)^{1/2}\left(\frac{(z-d)}{z^{2/3}}\right)^{1/2}\left(\frac{\phi_h(\varsigma)}{\tau u_*}\right)^{1/6} & z > z^* \\ \left(\frac{k}{\pi}\right)^{1/2}\frac{z^{2/3}}{\left(z^*\right)^{1/2}}\left(\frac{\phi_h(\varsigma)}{\tau u_*}\right)^{1/6} & h \le z \le z^* \end{cases} \tag{B1}$$

For a wide range of surface layer atmospheric conditions, equation (B1) is weakly dependent on the stability parameter through the stability function for heat due to its 1/6 power dependence. On the basis of ramp frequency scales with wind shear, *Chen et al.* [1997b] scaled $1/(\tau u_*)$ over z or $(z - d)$ in the roughness and inertial sublayers, respectively, through a constant parameter, λ. Here, the scale to analyze equation (B1) was used as a generalized form depending on the stability parameter, $\lambda_{(\zeta)}$,

$$\left[\alpha(k\beta)^2\right]^{1/3} = \begin{cases} \left(\frac{k}{\pi}\right)^{1/2}\left(\frac{(z-d)}{z}\right)^{1/3}\left(\lambda(\varsigma)\phi_h(\varsigma)\right)^{1/6} & z > z^* \\ \left(\frac{k}{\pi}\right)^{1/2}\left(\frac{z}{z^*}\right)^{1/2}\left(\lambda^*(\varsigma)\phi_h(\varsigma)\right)^{1/6} & h \le z \le z^* \end{cases} \tag{B2}$$

where parameters, $\lambda_{(\zeta)} = (z - d)/(\tau u_*)$ and $\lambda^*_{(\zeta)} = z/(\tau u_*)$, denote generalized scales corresponding for measurements made in the roughness and inertial sublayers, respectively.

[60] Figure B1 shows the scales $[\lambda_{(\zeta)}]^{1/3}$ and $[\lambda^*_{(\zeta)}]^{1/3}$ versus the stability parameter for each canopy and measurement levels, except for the nectarines campaign because the friction velocity was unavailable. Whether measurements were made in the roughness and inertial sublayers, both scales were rather insensitive to the stability conditions. When approximating to neutral and stable conditions its value becomes uncertain. Regardless of the measurement height above the canopy and type of canopy and according to these experimental results, it is proposed to approximate these scales to a constant value of 0.75 under unstable conditions that corresponds to a rounded value for $\zeta \le -0.025$ (Figure B1). When measuring close to the canopy top, *Paw U et al.* [1992] found the relationship: $1/\tau \sim a\, u_h/h$, where u_h is the wind speed at the canopy top with height h with $a \sim 0.11$ over different crops. Other values for $a \sim (0.11, 0.35)$ have also been reported depending on wind shear [*Shaw et al.*, 1995; *Raupach et al.*, 1996]. As a general rule, a reasonable relationship between friction velocity and wind speed measured in the roughness sublayer is as follows: $u_* \sim u_h/3$ [*Raupach et al.*, 1996], leading to the relationship for the scale, $\lambda^*_{(\zeta)} = h/(\tau u_*) \sim 3a \sim [0.33, 1.05]$. Therefore, because $[\lambda^*_{(\zeta)}]^{1/3} \sim [0.69,1.0]$, this interval is consistent with the proposed value for the scale $[\lambda^*_{(\zeta)}]^{1/3}$. *Chen et al.* [1997b] assumed the scale $\lambda^*_{(\zeta)}$ to be independent of ζ, $\lambda^*_{(\zeta)} = \lambda^*$, and from linear fit analysis, they obtained λ^* values of 0.4, 0.54 and 0.70, respectively, from data collected over bare soil at 0.03 m, straw mulch (0.06 m thick) at 0.09 m and Douglas fir Forest (16.7 m high) at 23 m. Therefore the scale $[\lambda^*]^{1/3} \sim [0.73, 0.88]$, is also in agreement with the values shown in Figure B1.

[61] Under unstable conditions, as a consequence of approximating the scales $\lambda_{(\zeta)}$ and $\lambda^*_{(\zeta)}$ as a constant from equation (B2), the dependence on the stability conditions attributed to the parameter $[\alpha(k\beta)^2]$ is through the relationship: $\phi_h^{1/2}(\zeta)$. Therefore, in equation (13), the total stability parameter dependence is through the stability function: $F_1(\zeta) = \phi_h^{-1/2}(\zeta)\, g_1^{-1/6}(\zeta)/(-\zeta)^{1/3}$. Similarly, sensible heat flux from equations (14) and (17) have a dependence on the stability parameter through the function, $F_2(\zeta) = \phi_h^{-1/2}(\zeta)\, g_2^{-1/3}(\zeta)/(-\zeta)^{1/3}$. Figure B2 shows the dependence on the stability parameter on functions $F_1(\zeta)$ and $F_2(\zeta)$. The functions show similar patterns and a weak dependence on the stability parameter for a wide range of unstable conditions indicating that the corresponding free convection limit is achieved under slightly unstable conditions. Small relative errors are introduced when the stability parameters are approximated as constants with values $F_1(\zeta) \sim F_2(\zeta) \sim 2.2$. For example, when the stability parameter ranges in the interval, $\zeta \le -0.1$, the respective mean relative errors obtained by this assumption are less than 10%. Equations (13), (14) and (17) therefore provide good estimates of sensible heat flux under unstable conditions and require only air temperature as an input.

[62] Under near-neutral conditions, $F_1(\zeta)$ and $F_2(\zeta)$ sharply increase but equations (13), (14) and (17) tend to zero as does the third-order structure function. Under stable conditions, one can approximate the stability functions $F_1(\zeta)$ and $F_2(\zeta)$ as constants for a wide range of the stability parameter: $1.0 \le \zeta$. Figure B2 shows, however, that the stability functions are highly dependent on the stability

parameter when $0 < \zeta \leq 1.0$. Such performance combined with the uncertainty of scales $\lambda_{(\zeta)}$ and $\lambda^*_{(\zeta)}$ point out the weakness for estimating sensible heat flux under stable conditions when only using air temperature measurements. Under very stable conditions (e.g., $1.0 < \zeta$), relationships based on Monin-Obukov similarity ($\phi_h(\zeta)$, $g_1(\zeta)$ and $g_2(\zeta)$) may be uncertain [*De Bruin et al.*, 1993]. It follows that equations (13), (14) and (17) hold under moderate stable conditions and that wind speed as well as temperature measurements are required because their stability parameter dependence.

[63] **Acknowledgments.** We gratefully acknowledge K. T. Paw U, M. Sugita, and three unknown reviewers for their useful, constructive, and competent suggestions. We thank Asun and Carla for their assistance; D. Spano for data from the experiments over grass, wheat, and grapevines; I. Ferreira for supporting the collection of data over the nectarine orchard in Portugal; J. Faci, M. Izquierdo, J. Gaudó, and D. Mayoral for their field assistance for the olive orchard experiment; and the owner of this orchard for his allowance of the experiment. We also thank the University of California, Davis, for providing facilities to analyze the data. This work was supported by the Ministerio de Ciencia y Tecnología under the Spanish projects REN2001-1630 CLI and TRANSCLA, the DURSI of the Generalitat of Catalunya and the University of Lleida. Data from the rangeland grass was supported by grants from the U.S. Department of Energy and the California Agricultural Experiment Station.

References

Allen, R. G., L. S. Pereira, D. Raes, and M. Smith (1998), Crop evapotranspiration: Guidelines for computing crop water requirements, *FAO Irrigat. Drain. Pap. 56*, 300 pp., Food and Agric. Org., Rome, Italy.

Allen, R. G., W. O. Pruitt, J. A. Businger, L. J. Fritschen, M. E. Jensen, and F. H. Quinn (1996), Evaporation and transpiration, in *Hydrology Handbook*, *ASCE Manual Rep. Eng. Practice*, vol. 28, 2nd ed., edited by R. J. Heggen, pp. 125–252, Am. Soc. of Civ. Eng., Reston, Va.

Anderson, F. E., R. L. Snyder, R. L. Miller, and J. Drexler (2003), A micrometeorological investigation of a restored California wetland ecosystem, *Bull. Am. Meteorol. Soc.*, *84*(9), 1170–1172.

Antonia, R. A., A. J. Chambers, and E. F. Bradley (1981), Temperature structure in the atmospheric surface layer II. The budget of mean cube fluctuations, *Bound Layer Meteorol.*, *20*, 293–307.

Baldocchi, D. D. (1997), Flux footprints within and over forest canopies, *Boundary Layer Meteorol.*, *85*, 273–292.

Baldocchi, D. D., X. Liukang, and N. Kiang (2004), How plant functional-type, weather, seasonal drought, and soil physical properties alter water and energy fluxes of an oak-grass savanna and an annual grassland, *Agric. For. Meteorol.*, *123*, 13–39.

Brutsaert, W. (1982), *Evaporation Into the Atmosphere*, 299 pp., Springer, New York.

Businger, J. A., J. C. Wyngaard, I. Izumi, and E. F. Bradley (1971), Flux profile relationships in the atmospheric surface layer, *J. Atmos. Sci.*, *28*, 181–189.

Castellví, F. (2004), Combining surface renewal analysis and similarity theory: A new approach for estimating sensible heat flux, *Water Resour. Res.*, *40*, W05201, doi:10.1029/2003WR002677.

Castellví, F., and A. Martínez-Cob (2005), Estimating sensible heat flux using surface renewal analysis and the variance method. A study case over olive trees at Sstago (NE, Spain), *Water Resour. Res.*, *41*, W09422, doi:10.1029/2005WR004035.

Castellví, F., P. J. Perez, and M. Ibañez (2002), A method based on high-frequency temperature measurements to estimate the sensible heat flux avoiding the height dependence, *Water Resour. Res.*, *38*(6), 1084, doi:10.1029/2001WR000486.

Cellier, P. (1986), On the validity of flux-gradient relationships above very rough surfaces, *Boundary Layer Meteorol.*, *36*, 417–419.

Cellier, P., and Y. Brunet (1992), Flux-gradient relationships above tall plant canopies, *Agric. For. Meteorol.*, *58*, 93–117.

Chen, W., M. D. Novak, T. A. Black, and X. Lee (1997a), Coherent eddies and temperature structure functions for three contrasting surfaces. part I: Ramp model with finite micro-front time, *Boundary Layer Meteorol.*, *84*, 99–123.

Chen, W., M. D. Novak, T. A. Black, and X. Lee (1997b), Coherent eddies and temperature structure functions for three contrasting surfaces. part II: Renewal model for sensible heat flux, *Boundary Layer Meteorol.*, *84*, 125–147.

De Bruin, H. A. R., N. J. Bink, and L. J. M. Kroon (1991), Fluxes in the surface layer under advective conditions, in *Land Surface Evaporation: Measurement and Parameterization*, edited by T. J. Schmugge and J. C. André, pp. 157–171, Springer, New York.

De Bruin, H. A. R., W. Kohsiek, and B. J. J. M. Van Den Hurk (1993), A verification of some methods to determine the fluxes of momentum, sensible heat and water vapor using standard deviation and structure parameter of scalar meteorological quantities, *Boundary Layer Meteorol.*, *65*, 231–257.

Duce, P., D. Spano, and R. L. Snyder (1998), Effect of different fine-wire thermocouple design on high frequency temperature measurements, paper presented at AMS 23rd Conference on Agricultural and Forest Meteorology, Alburqueque, N. M.

Garrat, J. R. (1980), Surface influence upon vertical profiles in the atmospheric near-surface layer, *Q. J. R. Meteorol. Soc.*, *106*, 803–819.

Higbie, R. (1935), The rate of absorption of a pure gas into a still liquid during short periods of exposure, *Trans. Am. Inst. Chem. Eng.*, *31*, 365–388.

Högström, U. (1990), Analysis of turbulent structure in the surface layer with a modified similarity formulation of near neutral conditions, *J. Atmos. Sci.*, *47*, 1949–1972.

Hsieh, C., G. G. Katul, J. Schieldge, J. Sigmon, and K. R. Knoerr (1996), Estimation of momentum and heat fluxes using dissipation and flux-variance methods in the unstable surface layer, *Water Resour. Res.*, *32*(8), 2453–2462.

Kaimal, J. C., and J. J. Finnigan (1994), *Atmospheric Boundary Layer Flows, Their Structure and Measurement*, 289 pp., Oxford Univ. Press, New York.

Katul, G., M. Goltz, C. Hsieh, Y. Cheng, F. Mowry, and J. Sigmon (1995), Estimation of surface heat and momentum fluxes using the flux-variance method above uniform and non-uniform terrain, *Boundary Layer Meteorol.*, *74*, 237–260.

Katul, G., C. Hsieh, R. Oren, D. Ellsworth, and N. Philips (1996), Latent and sensible heat flux predictions from a uniform pine forest using surface renewal and flux variance methods, *Boundary Layer Meteorol.*, *80*, 249–282.

Kormann, R., and F. X. Meixner (2001), An analytical footprint model for non-neutral stratification, *Boundary Layer Meteorol.*, *99*, 207–224.

Lloyd, C. R., A. D. Culf, A. J. Dolman, and J. H. C. Gash (1991), Estimates of heat flux from observations of temperature observations, *Boundary Layer Meteorol.*, *57*, 311–322.

Paw U, K. T., Y. Brunet, S. Collineau, R. H. Shaw, T. Maitani, J. Qiu, and L. Hipps (1992), On coherent structures in turbulence within and above agricultural plant canopies, *Agric. For. Meteorol.*, *61*, 55–68.

Paw U, K. T., J. Qiu, H. B. Su, T. Watanabe, and Y. Brunet (1995), Surface renewal analysis: A new method to obtain scalar fluxes without velocity data, *Agric. For. Meteorol.*, *74*, 119–137.

Paw U, K. T., R. L. Snyder, D. Spano, and H. B. Su (2005), Surface renewal estimates of scalar exchanges, *Micrometeorology in Agricultural Systems*, *Agron. Monogr.*, vol. 47, pp. 445–484, ASA-CSSA-SSSA, Madison, Wisc.

Raupach, M. R., J. J. Finnigan, and Y. Brunet (1996), Coherent eddies and turbulence in vegetation canopies: The mixing-layer analogy, *Boundary Layer Meteorol.*, *78*, 351–382.

Sellers, P. J., Y. Mintz, Y. C. Sud, and A. Dalcher (1986), A simple biosphere model (SiB) for use within general circulation models, *J. Atmos. Sci.*, *43*, 505–531.

Shaw, R. H. (2002), Flow above and within the canopy, in *Advanced Short Course on Agricultural, Forest and Micrometeorology*, *Lecture 20*, 30 pp. 3, Consig. Naz. delle Ric., Sassari, Italy.

Shaw, R. H., Y. Brunet, J. J. Finnigan, and M. R. Raupach (1995), A wind tunnel study of air flow in waving wheat: Two-point velocity statistics, *Boundary Layer Meteorol.*, *76*, 349–376.

Snyder, R., D. Spano, and K. T. Paw U (1996), Surface renewal analysis for sensible and latent heat flux density, *Boundary Layer Meteorol.*, *77*, 249–266.

Spano, D., R. L. Snyder, P. Duce, and K. T. Paw U (1997), Surface renewal analysis for sensible heat flux density using structure functions, *Agric. For. Meteorol.*, *86*, 259–271.

Spano, D., R. L. Snyder, and K. T. Paw U (2000), Estimating sensible and latent heat flux densities from grapevine canopies using surface renewal, *Agric. Forest Meteorol.*, *104*, 171–183.

Stull, R. B. (1991), *An Introduction to Boundary Layer Meteorology*, 666 pp., Springer, New York.

Tillman, J. E. (1972), The indirect determination of stability, heat and momentum fluxes in the Atmospheric boundary layer from simple scalar variables during dry unstable conditions, *J. Appl. Meteorol.*, *11*, 783–792.

Van Atta, C. W. (1977), Effect of coherent structures on structure functions of temperature in the atmospheric boundary layer, *Arch. Mech.*, *29*, 161–171.

Weaver, H. L. (1990), Temperature and humidity flux-variance relations determined by one-dimensional eddy correlation, *Boundary Layer Meteorol.*, *53*, 77–91.

Wesson, K. H., G. Katul, and C.-T. Lai (2001), Sensible heat flux estimation by flux variance and half-order time derivative methods, *Water Resour. Res.*, *37*(9), 2333–2343.

Willmott, C. J. (1982), Some comments on the evaluation of model performance, *Bull. Am. Meteorol. Soc.*, *63*(11), 1309–1313.

Wyngaard, J. C., Y. Izumi, and S. A. Collins (1971), Behavior of the refractive-index structure parameter near the ground, *J. Opt. Soc. Am.*, *61*, 1646–1650.

Zapata, N., and A. Martínez-Cob (2001), Estimation of sensible and latent heat flux from natural sparse vegetation surfaces using surface renewal, *J. Hydrol.*, *254*, 215–228.

D. D. Baldocchi, Department of Environmental Science, Policy and Management, University of California, 137 Mulford Hall, Berkeley, CA 94720-0000, USA.

F. Castellví, Departamento de Medi Ambient i Cienciès del Sòl, University of Lleida, ETSEA Rovira Roure, 191, Lleida E-25198, Spain. (f-castellvi@macs.udl.es)

A. Martínez-Cob, Departamento de Genética y Producción Vegetal, Estación Experimental de Aula Dei, Consejo Superior de Investigaciones Científicas, Apartado 202, Zaragoza, E-50080, Spain.

R. L. Snyder, Department of Land, Air and Water Resources, University of California, One Shields Avenue, Davis, CA 95616-8627, USA.